Regulating crystal facets of MnO_2 for enhancing peroxymonosulfate activation to degrade pollutants: Performance and mechanism

Juncong Fu [a,l], *Peng Gao* [b,l], *Lu Wang* [a], *Yongqing Zhang* [a,c,d,*], *Yuhui Deng* [a], *Renfeng Huang* [a], *Shuaifei Zhao* [e], *Zebin Yu* [f], *Yuancheng Wei* [g], *Guangzhao Wang* [h], *Shaoqi Zhou* [i]

[a] *School of Environment and Energy, Guangdong Provincial Key Laboratory of Atmospheric Environment and Pollution Control, South China University of Technology, Guangzhou 510640, China.*

[b] *School of Chemistry and Molecular Bioscience, University of Wollongong, NSW 2500, Australia.*

[c] *The Key Lab of Pollution Control and Ecosystem Restoration in Industry Clusters, Ministry of Education, Guangzhou 510006, China.*

[d] *State Key Laboratory of Pulp and Paper, South China University of Technology, Guangzhou*

[e] *Institute for Frontier Materials, Deakin University, Geelong, Victoria, 3216, Australia*

[f] *School of Resources, Environment and Materials, Guangxi University, Nanning 530004 Guangxi, P.R. China*

[g] *Preliminary Work Management Center for Government Investment Project of Shenzhen Longhua District*

[h] *Key Laboratory of Extraordinary Bond Engineering and Advanced Materials Technology of Chongqing, School of Electronic Information Engineering, Yangtze Normal University*

[i] *Guizhou Academy of Sciences, Shanxi Road 1, Guiyang, 550001, China*

[l] *These authors contributed equally to this work.*

* Corresponding author: Yongqing Zhang

Tel: +86 13434389968

Fax: +86-20-39380508

E-mail address: zhangyq@scut.edu.cn

Text S1 DFT Calculation Method.

The density functional theory (DFT) calculations were performed using the Vienna Ab initio Simulation Package (VASP) with plane wave basis sets and projector-augmented wave (PAW) pseudopotentials [1-3]. The generalized gradient approximation (GGA) of the Perdew–Burke–Ernzerhof functional (PBE) with Hubbard *U* corrections was used for all geometry optimizations and energy calculations [4, 5]. The planewave cut-off energy was set to 500 eV and *U*=1.6 eV [6]. For calculations of bulks, the (3 × 3 × 3) Monkhorst−Pack meshes were used for the k-point samplings [7]. To study the slab model, the thickness of the vacuum layer along the z-direction was set to 15 Å to ensure negligible interactions between the slab surfaces due to periodic boundary conditions. Calculation convergence thresholds for the electronic structure and forces were set to be 10^{-5} eV and 0.02 eV $Å^{-1}$, respectively. The adsorption energy (E_{ads}) of PMS molecules on facet-engineered α-MnO_2 was calculated as follows [8]:

$$E_{ads} = E_{total} - E_{basic} - E_{molecule} \quad (1)$$

where E_{ads} means the adsorption energy of PMS molecule, E_{total} means the total energy of the surface with PMS, E_{basic} represent the total energy of the surface without PMS, and $E_{molecule}$ is the energy of PMS.

Text S2 Reagents used in the experiment.

p-Chloroaniline (PCA, > 99.5%), 5,5-Dimethyl-1-pyrroline N-oxide (DMPO, 97.0%), Potassium iodide (KI, > 99.0%), 4-Hydroxy-2,2,6,6-tetramethylpiperidine (TEMP, > 99.0%), tert-butanol (TBA, > 99.0%), furfuryl alcohol (FFA, > 98.0%), methanol (MeOH, HPLC), sodium thiosulfate pentahydrate ($Na_2S_2O_3$•$5H_2O$, > 99.0%), sodium bicarbonate ($NaHCO_3$, >99.0%), ethanol (EtOH), Rhodamine B (RhB, AR), ammonium oxalate monohydrate ($(NH_4)_2C_2O_4$•H_2O, > 99.8%), ammonium sulfate ($(NH_4)_2SO_4$, > 99.0%), manganese sulfate monohydrate ($MnSO_4$•H_2O, > 99.0%), ammonium persulfate ($(NH_4)_2S_2O_8$, > 98.0%), humic acid (HA, ≥ 90.0%), phenol (> 99.0%), *p*-Benzoquinone (*p*-BQ, > 99.0%), 4-Mercaptobenzoic acid (> 90.0%) were purchased from Shanghai Aladdin Chemistry Inc., China. Imidacloprid (IMI, AR) was purchased from Yuanye Biotechnology Company (Shanghai China). Sodium hydroxide (NaOH, ≥ 98%), sodium nitrate ($NaNO_3$, > 99.0%), sodium perchlorate ($NaClO_4$, > 99.0%) were purchased from Tianjin Kemiou Chemical Reagent Co., Ltd., China. Potassium permanganate ($KMnO_4$, ≥ 99.5%), potassium nitrate (KNO_3, > 99.0%), sulfuric acid (H_2SO_4, ≥ 98%) were purchased from Guangzhou chemical reagent factory. Tetracycline hydrochloride (TC, > 96.0%), potassium monopersulfate triple salt (PMS, > 42%), sodium sulfate anhydrous (Na_2SO_4, > 99.0%), sodium nitrite ($NaNO_2$, > 99.0%) were purchased from Macklin Biochemical Technology Co., Ltd, China. Sodium chloride (NaCl, > 99.5%) was purchased from Tianjin Damao Chemical Reagent Factory, China. Deionized water was made by Milli-Q System and used for all experiments.

Text S3 Experimental sample preparation.

TOC sample preparation. During the degradation experiment, 5 mL of the reaction filter liquor was taken at given time intervals and added to a 50 mL centrifuge tube containing 10 mL of $NaNO_2$ (50 mM) for the TOC test.

EPR sample preparation. For the radicals capture test, 0.5 mL of 2 mol/L DMPO was added to 9.5 mL of the reaction mixture, and samples were taken for EPR analysis after 3 min. For the singlet oxygen capture test, 0.5 mL of 200 mmol/L TEMP was added to 9.5 mL of the reaction mixture, and samples were taken for EPR analysis after 3 min.

Cyclic voltammetry (CV) curves. 10 mg of catalyst was mixed with 1 mL of ethanol, then 0.5 mL of Nafion solution was added. To completely disperse the catalyst into liquid, the mixture was sonicated for 15 min. Then, 5 μL of the mixed solution was dropped on the surface of the polished glassy carbon electrode and allowed to dry naturally. Silver/silver chloride electrode (Ag/AgCl) and Pt wire electrode were used as reference electrode and counter electrode, respectively. CV curves were measured at the potential from 0.0 - 1.5 V (vs. Ag/AgCl) with a scanning rate of 50 mV/s with 100 mmol/L Na_2SO_4 as supporting electrolyte.

Sulfhydryl modification steps. 25 mg of catalyst was dispersed in 100 mL of 10 mmol/L 4-Mercaptobenzoic acid under magnetic stirring for 24 h [9]. FTIR spectra were used to verify whether the modification was successful.

Table. S1. Properties of the three MnO_2 catalysts

Sample	$S_{BET}/(m^2/g)$	Total pore volume/(cm^3/g)	Average pore diameter/(nm)
100-MnO_2	67.8	0.56	32.8
110-MnO_2	104.9	0.69	26.3
310-MnO_2	116.0	0.53	18.2

Table. S2. Chemical and surface compositions of facet engineered MnO_2 before and after the reaction

samples	Mn^{2+} (%)	Mn^{3+} (%)	Mn^{4+} (%)	O_{latt} (%)	O_{ads} (%)	$Mn^{2+}+Mn^{3+}/Mn^{4+}$	O_{ads}/O_{latt}	AOS[a]
100-MnO_2	7.05	36.57	56.38	65.19	34.81	0.77	0.53	3.53
110-MnO_2	7.43	37.95	54.62	70.20	29.80	0.83	0.42	3.55
310-MnO_2	6.55	37.66	55.79	69.19	30.81	0.79	0.45	3.55
310-MnO_2 (After reaction)	7.68	35.03	57.29	68.67	31.33	0.75	0.46	3.57

[a]The average oxidation state (AOS) of Mn was calculated by the equation AOS=8.956-1.126ΔE (ΔE is the binding energy difference of Mn 3*s*) [10].

Table. S3. Analytical details for organic compounds by HPLC

Organics	Mobile phase (A/B)	Ratio of A/B (v/v)	Detective wavelength (nm)	Flow rate (mL/min)
PCA	methanol/H_2O	70/30	254	0.7
phenol	methanol/H_2O	70/30	270	0.8
IMI	acetonitrile/H_2O	70/30	270	0.7

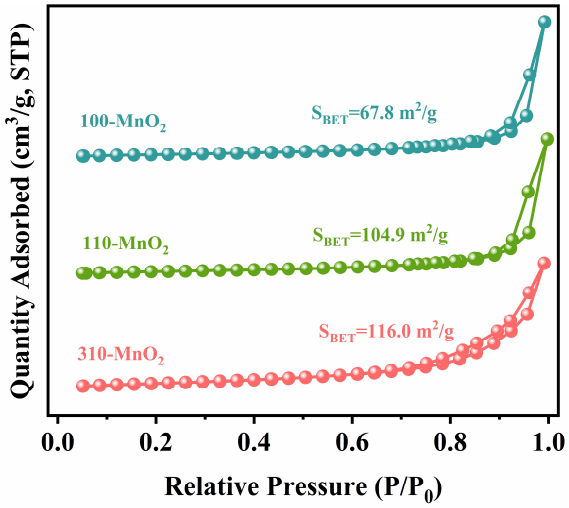

Fig. S1 The N_2 adsorption/desorption isotherms of the three MnO_2 catalysts.

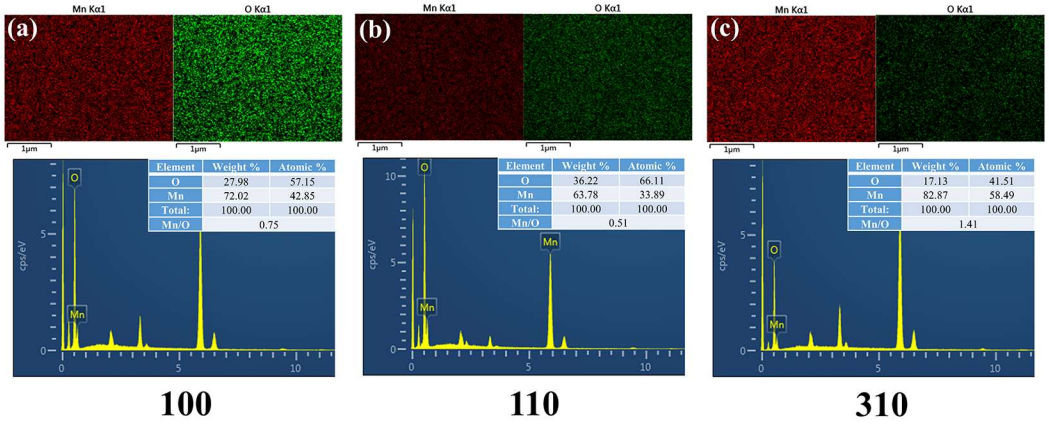

Fig. S2 EDS-mapping images of (a) 100-MnO_2, (b) 110-MnO_2, and (c) 310-MnO_2.

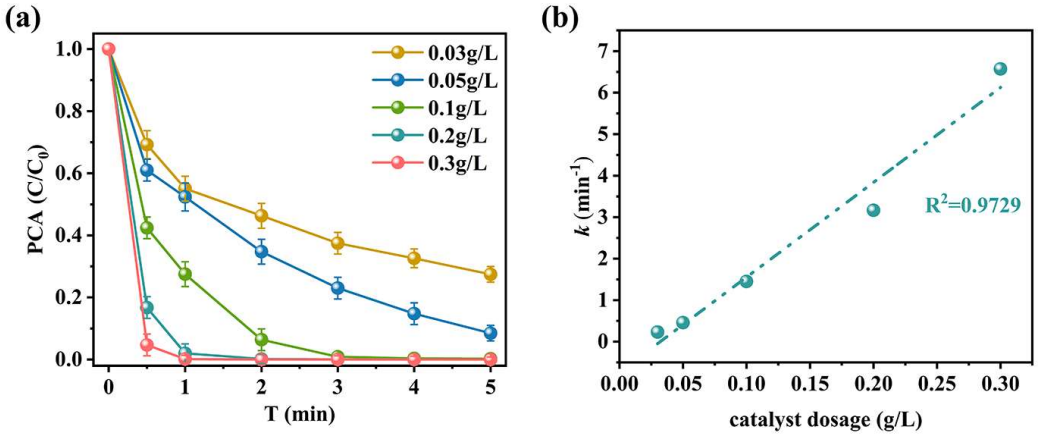

Fig. S3 (a) Effect of MnO_2 dosage in 310-MnO_2/PMS system and (b) correlation of the rate constants to the MnO_2 dosage, reaction conditions: $[PCA]_0$ = 1.0 mmol/L, $[PMS]_0$ = 1.5 mmol/L, $[MnO_2]_0$ = 0.03-0.3 g/L, without pH adjustment.

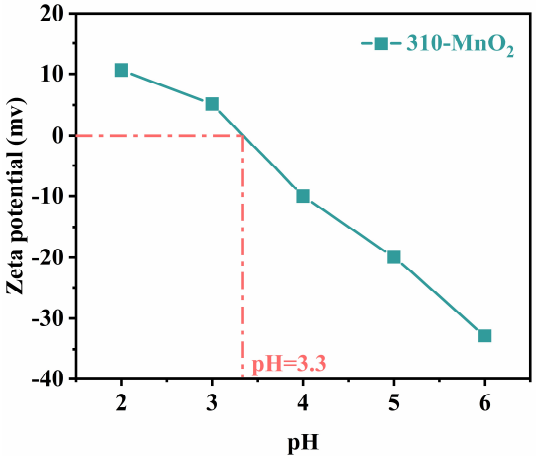

Fig. S4 The zeta potential curves of the 310-MnO_2, test conditions: $[MnO_2]_0$ = 0.1 g/L.

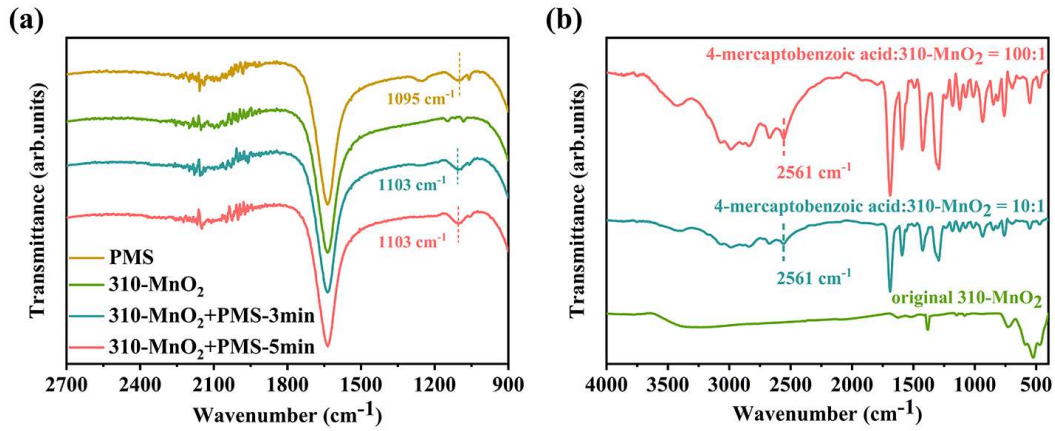

Fig. S5 (a) ATR-FTIR spectra demonstrating the PMS complexation on the catalyst surface, reaction conditions: $[PMS]_0$ = 60 mmol/L, $[MnO_2]_0$ = 4 g/L, without pH adjustment; (b) ATR-FTIR spectra of 310-MnO_2 solid before and after modifying with -SH group.

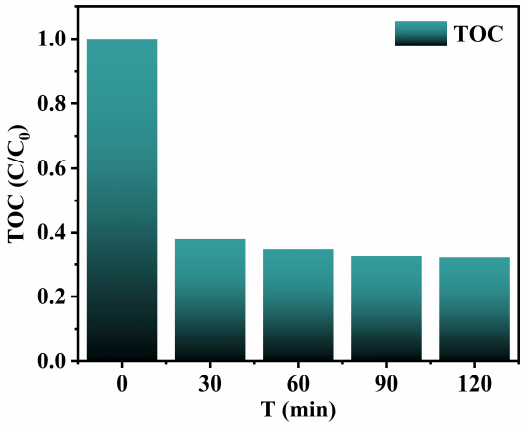

Fig. S6 TOC removal of PCA degradation with 310-MnO_2/PMS system, reaction conditions: $[PCA]_0$ = 1.0 mM, $[PMS]_0$ = 1.5 mM, $[MnO_2]_0$ = 0.1 g/L, without pH adjustment.

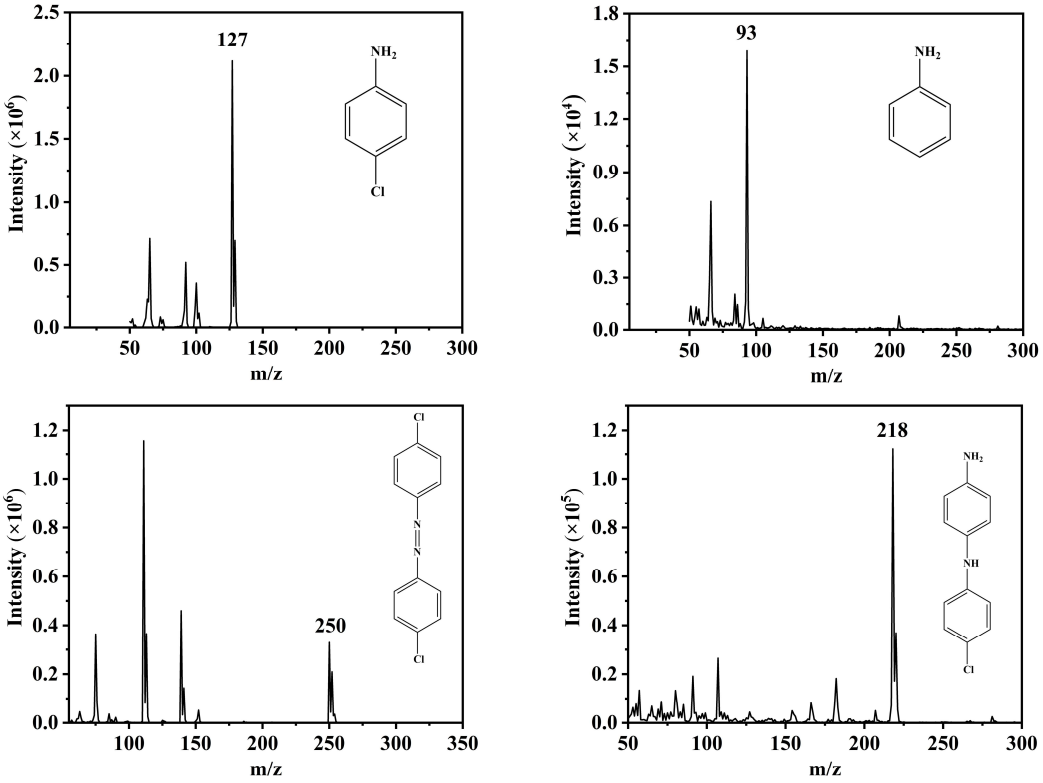

Fig. S7 Mass spectra and proposed structure of possible intermediate products.

References:

1. W. Kohn, L.J. Sham, Self-Consistent Equations Including Exchange and Correlation Effects, Phys. Rev. 140(4A) (1965) A1133-A1138. https://doi.org/10.1103/PhysRev.140.A1133.
2. G. Kresse, J. Furthmuller, Efficiency of ab-initio total energy calculations for metals and semiconductors using a plane-wave basis set, Comput. Mater. Sci. 6(1) (1996) 15-50. https://doi.org/10.1016/0927-0256(96)00008-0.
3. G. Kresse, D. Joubert, From ultrasoft pseudopotentials to the projector augmented-wave method, Phys. Rev. B 59(3) (1999) 1758-1775. https://doi.org/10.1103/PhysRevB.59.1758.
4. J.P. Perdew, K. Burke, M. Ernzerhof, Generalized Gradient Approximation Made Simple, Phys. Rev. Lett. 77(18) (1996) 3865-3868. https://doi.org/10.1103/PhysRevLett.77.3865.
5. G.A.E. Oxford, A.M. Chaka, First-Principles Calculations of Clean, Oxidized, and Reduced beta-MnO2 Surfaces, J. Phys. Chem. C 115(34) (2011) 16992-17008. https://doi.org/10.1021/jp2037137.
6. Y. Crespo, N. Seriani, A lithium peroxide precursor on the alpha-MnO2 (100) surface, J. Mater. Chem. A 2(39) (2014) 16538-16546. https://doi.org/10.1039/c4ta02658f.
7. H.J. Monkhorst, J.D. Pack, Special points for Brillouin-zone integrations, Phys. Rev. B 13(12) (1976) 5188-5192. https://doi.org/10.1103/PhysRevB.13.5188.
8. J. Yu, T. Zeng, H. Wang, H. Zhang, Y.P. Sun, L. Chen, S. Song, L.X.Y. Li, H.X. Shi, Oxygen - defective MnO_{2-x} rattle-type microspheres mediated singlet oxygen oxidation of organics by peroxymonosulfate activation, Chem. Eng. J. 394 (2020) 124458. https://doi.org/10.1016/j.cej.2020.124458.
9. X. Du, Y. Zhang, F. Si, C. Yao, M. Du, I. Hussain, H. Kim, S. Huang, Z. Lin, W. Hayat, Persulfate non-radical activation by nano-CuO for efficient removal of chlorinated organic compounds: Reduced graphene oxide-assisted and CuO (001) facet-dependent, Chem. Eng. J. 356 (2019) 178-189. https://doi.org/10.1016/j.cej.2018.08.216.
10. Y. Yang, J. Huang, S. Wang, S. Deng, B. Wang, G. Yu, Catalytic removal of gaseous unintentional POPs on manganese oxide octahedral molecular sieves, Appl. Catal. B 142 (2013) 568-578. https://doi.org/10.1016/j.apcatb.2013.05.048.